



Parametric Analysis for Torque Prediction in Friction Stir Welding Using Machine Learning and Shapley Additive Explanations

Sif Eddine Belalia^{a, b}, Mohamed Serier^{c,*}, Raheem Al-Sabrah^d

^a *Departement of Mechanical Engineering, University of Relizane, Relizane, 48000, Algeria*

^b *Industrial Engineering and Sustainable Development Laboratory, Faculty of Science and Technology, University of Relizane, Relizane, Algeria*

^c *Departement of Mechanical Engineering, University of Ain Témouchent Belhadj Bouchaib, Ain Témouchent, Algeria*

^d *Mechanical Department, Engineering College, University of Basrah, Basrah, Iraq*

Abstract

Friction Stir Welding (FSW) has revolutionized modern manufacturing with its advantages, such as minimal heat-affected zones and improved material properties. Accurate torque prediction in FSW is crucial for weld quality, process efficiency, and energy conservation. Many researchers achieved models for torque based on experimental research, yet the models were limited to a specific type of material. In recent years, the use of machine learning techniques has increased in industry in general and in welding in particular. In this study, a machine learning model was prepared based on artificial neural networks, and Shapley-Additive Explanations were used to predict the rotational torque from 287 experiments that had been conducted in several previous studies. The achieved model has remarkable predictive performance, with an R-squared of 99.53% and low errors (MAE, MAPE, and RMSE). Moreover, a machine learning polynomial regression was examined for comparisons. A parametric importance analysis revealed that rotational speed, plate thickness, and tilt angle significantly affect torque predictions, while the rest of the variables had minimal importance.

Keywords: Friction stir welding; torque prediction; Artificial neural network; Parametric study; Shapley Additive Explanations

1. Introduction

Machine learning is a unique technique branching from artificial intelligence, based on enabling computers, through specific algorithms, to learn from available data and be able to predict outcomes [1]. In the last decade, machine learning has emerged as a successful tool in improving the performance of many industries [2, 3]. It has undoubtedly contributed to achieving the optimal values for the inputs to obtain the highest possible efficiency [4]. Machine learning is one of many methods used for modeling, analyzing [5-7] and optimizing [8-10] engineering and

* Corresponding author: *E-mail address:* belalia.sifeddine@univ-relizane.dz

science[11] problems. Researchers and users of welding machines are not late in investing in the capabilities of machine learning in analyzing data and creating advanced algorithms in many processes, especially in fusion welding such as laser welding [12], arc welding [13, 14], and spot welding [15, 16]. In addition, solid state welding has also benefited from machine learning techniques such as ultrasonic welding [17] and friction stir welding [18].

In the late 1990s, friction stir welding (FSW) was invented as a solid-state welding method [19, 20]. During the FSW process, as shown in Fig 1, two plates of similar or dissimilar metals are joined by passing a non-consumable tool that rotates at a certain rotational speed until plastic deformation begins to occur between the two plates. Then, the tool moves at a transverse speed along the area to be welded, and then the tool rises, leaving a hole at the end of the welded area[21, 22].

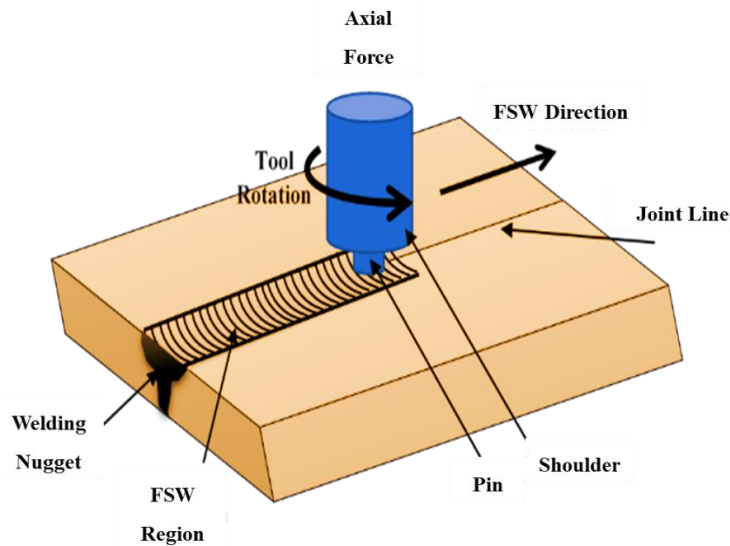


Fig 1: Friction stir welding process and tool parts

In recent years, the use of FSW has expanded steadily, and it has become capable of welding dissimilar metals, such as aluminum to copper [23, 24] and magnesium to copper [25]. It has even surprised many researchers with its ability to weld metals with melting points far apart, such as welding magnesium to steel [26, 27]. The high ability to weld metals demonstrated by FSW processes opened the door to more unconventional processes, such as welding similar or dissimilar polymers [28, 29] or welding polymers to metals [30]. The results were original and very encouraging.

The rotational speed and transverse velocity of the tool, in addition to the tool geometry, especially shoulder diameter, pin profile, plunge depth, and tilt angle, are considered the most influential input parameters in the FSW process, as shown in Fig 2 [31, 32]. Torque is an indicator for applying load during FSW, and it is an essential quantity and has an impact on the welding quality. Accurate torque prediction in FSW affects heat generation, material softening and plasticizing, stirring action, penetration depth, process stability, and parameter optimization. In other words, by controlling torque, heat generation during welding is effectively managed, influencing the material flow and, consequently, the mechanical properties of the weld. This control not only enhances weld quality but also prevents excessive tool wear, extending the lifespan of valuable FSW equipment and significantly lowering energy costs, contributing to both economic and environmental sustainability while maintaining superior welding outcomes.



Fig 2: Main parameters of the FSW process

Several studies dealt with torque measurements during FSW processes. S. Cui et al. [33] studied the effect of rotational speed and forward speed on torque when welding A356 aluminum alloy using FSW. They prepared a linear model to describe the relationship between them that allows for a detailed evaluation of torque sensitivity to these inputs. J W Qian et al. [34] revealed that the torque and the fraction of slipping exhibit variations with an identical periodicity, precisely matching the time taken for a single rotation of the tool for FSW of commercial aluminum alloy (AA1100-H14). Aluminum alloys containing copper, such as AA2024, have been the focus of studies by several researchers to find torques, such as L. Shi et al. [35], and Pew et al. [36], who used AA2024-T3, while Su & Wu used AA2024-T4 [37]. The effects of torque on the nugget and heat-affected zone regions in this class of alloys when using FSW were studied by Junhui Yan et al. [38]. The most extensive study of torque calculations for this type of alloy was done by Long et al. [39]. Although the study focused on AA2219-T87, it included comparisons with aluminum alloys of other categories, such as AA5083-O and AA7050-T751. Torque in FSW has been the focus of study by many researchers using the superior hardener Aluminum 5xxx alloys, which are strengthened with magnesium, such as AA5083-O [39], AA5754 [40], and AA5052-H34 alloy [41-43]. The strength-to-weight ratio provided by AA6XXX alloys, along with their improved mechanical properties, has emerged as a critical set of criteria, so these alloys are widely used in FSW, including torque measurements such as AA6061-T6 [44-48] and AA6092. Finally, Torque measurements of extruded wrought aluminum alloy AA7xxx based on manganese content showed that these alloys can withstand high torques, especially AA7050-T7451 [47, 49] and AA7075-T6 [50, 51], in addition to AA7039 [50] alloy. Torque studies were not limited to welding similar alloys but rather extended to include dissimilar alloys, especially aluminum alloys, such as joining AA5083-130 HV and AA6082-T6 [52], as well as joining AA6061-T6 and AA5083-H111 [53].

Despite the importance of torque in FSW operations, studies that discuss this importance are still limited and do not give a unified view of the importance of torque or methods for predicting it. Therefore, there are research gaps and points that need to be highlighted. The current study chose a unique approach to studying torque and the possibility of predicting it through parametric analysis of previous studies based on harnessing the power of machine learning, specifically artificial neural networks (ANN). This approach is considered a departure from traditional methods, as it is possible to understand the complex relationships between the various input parameters and torque. This study investigates both similar and dissimilar aluminum alloys.

2. Materials and Methods

2.1. Experimental Studies

The current study was built based on data from 287 experiments conducted in 22 previous studies for aluminum alloys, as shown in Table 1. The study included the most used categories in FSW studies, which are AA1xxx, AA2xxx, AA5xxx, and AA5xxx alloys with different heat treatment ranges.

Notably, the data pool exhibited a mixed nature, with numeric data complemented by values extracted from graphical representations. The dataset contains experiments on similar and dissimilar plates. All pins are either cylindrical or conical in shape. A type of correlation was used to overcome the lack of pin length in several studies. A distinctive feature of the dataset was the replacement of pin-related attributes. The dataset's summary statistics in Table 2 offer insights into the dataset's distribution and central tendencies, where T is torque, RS is the rotation speed of the tool, and WS is velocity. R1, R2, and R3 are the radius of the shoulder, pin base, and pin tip, respectively. L0 is plate thickness, L1 is the tool's pin length, and Alpha represents the tilt angle. The AS TS and RS TS are the tensile strengths of the advancing and retreating plate sides, respectively.

Table 1: Welding configurations of the examined studies

Exp. ID	Plates Material	Plate thickness (mm)	Source
1	A356 (Al-7Si-0.3Mg)	6.4	[33]
2	AA1100-H14	8.0	[34]
3	AA2024-T3	6.0	[35]
4	AA2024-T3	9.5	[36]
5	AA2024-T4	5.9	[37]
6	AA2219-T87	8.3	[39]
7	AA2524-T351	6.4	[38]
8	AA5052-H34	5.0	[41-43]
9	AA6092/17.5 SiCp-T6 composite	6.0	[48]
10	AA7039	9.5	[50]
11	AA7050-T7451	32.0	[47]
12	AA7050-T7451	6.4	[49]
13	AA7050-T751	9.5	[39]
14	AA7075-T6	9.5	[50]
15	AA7075-T6	6.3	[50]
16	AA7075-T6	3.5	[51]
17	AA5083-O	9.5	[39]
18	AA5754	2.0	[40]
19	AA6061-T6	6.0	[44-45]
20	AA6061-T6	4.7	[46]
21	AA6061-T651	25.0	[47]
Dissimilar materials			
22	AA5083-130 HV/AA6082-T6	3.0	[52]
23	AA6082-T6/AA5083-130 HV	3.0	[52]
24	AA6061-T6/AA5083-H111	3.0	[53]

2.2. Methodology

In pursuit of this objective, this paper is built upon creating a deep learning neural network model (ANN), which is a machine learning method of modeling known for its ability to find complex and non-linear relations between

variables [54]. Furthermore, SHAP (Shapley Additive exPlanations) is used to interpret the output of our ANN model.

2.2.1. Artificial Neural Network (ANN) Model

The neural network model, with its architecture illustrated in Fig 3, is the heart of this research. It was designed and trained to predict torque values based on a comprehensive set of input features. The model architecture is constructed using Python scripts and libraries like TensorFlow and Keras. The model comprises multiple layers. Standardization of the feature set was implemented using StandardScaler to ensure consistent scaling across variables.

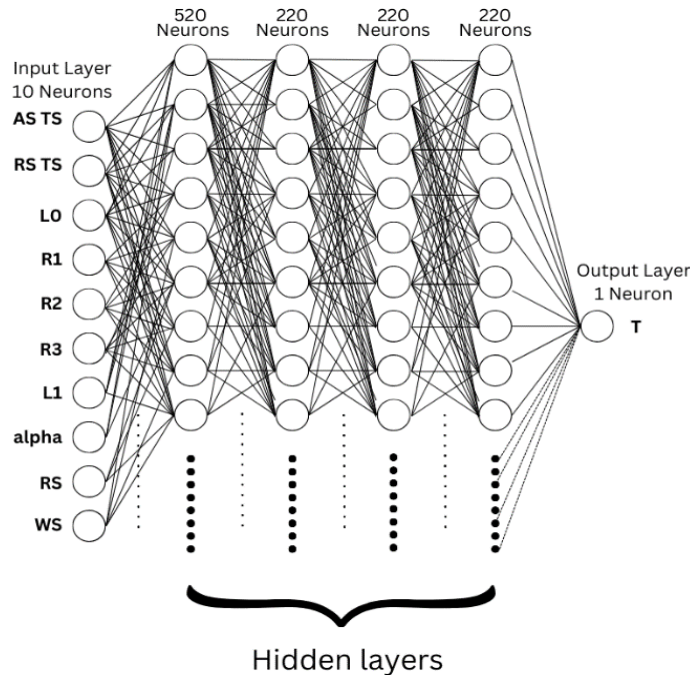


Fig 3: Architecture of the ANN model

There is a first dense layer with 520 neurons and a rectified linear unit (ReLU) activation function in the neural network architecture. After that, three hidden layers were added, and each one had 220 neurons activated by ReLU. Empirical findings during model development served as a guide for choosing these layer sizes, with a focus on balancing model complexity and generalization performance. The output layer consists of a single neuron responsible for predicting torque values.

For optimization, the Adam optimizer was employed. The loss function chosen was mean squared error (MSE), aligning with the objective of minimizing the difference between predicted and actual torque values. During training, the model was subjected to 700 epochs with a batch size of 276. Early experimentation revealed that a validation split of 20% yielded optimal results, enabling the model to generalize effectively while avoiding overfitting.

A Python script was employed to partition it into training, validation, and test sets. Specifically, the data was divided into feature variables (X) and a target variable (y). The training and validation data, constituting 70% of the dataset, were separated from the test data (30%) using the `train_test_split` function, with a random state of 70 to ensure reproducibility. The statistics of the experimental data used for training, testing, and validating the ANN model are shown in Table 2.

Table 2: Statistics data used to train, test, and validate the ANN model

modal parameters	mean	std	min	25%	50%	75%	max
AS TS	371.05	130.68	133.96	262.00	326.00	492.00	567.00
RS TS	370.58	131.00	133.96	262.00	326.00	492.00	567.00

L0	10.82	9.44	2.00	5.00	6.40	9.50	32.00
R1	10.12	3.09	5.00	7.50	10.00	12.70	17.50
R2	4.03	1.61	1.50	3.00	3.55	6.00	6.25
R3	3.48	1.73	1.25	2.00	3.00	5.00	6.25
L1	7.56	4.64	1.20	4.00	6.00	9.35	15.90
alpha	1.25	1.19	0.00	0.00	2.00	2.50	3.00
WS	184.51	263.67	28.00	76.20	102.00	202.92	1800.00
RS	646.28	500.47	52.41	265.00	549.73	900.00	2800.00
T	88.09	96.15	6.18	14.87	48.56	105.92	340.49

2.2.2. Artificial Shapley Additive exPlanations (SHAP)

For interpreting the output of our ANN model, we used SHAP (Shapley Additive exPlanations) [55]. SHAP is an interpreting model based on game theory [56] and local explanations [57]; it offers a means to estimate the contribution of each feature. Assuming an ANN model where a group N (with n features) is used to predict an output (N). In SHAP, the contribution of each feature (φ_i is the contribution of feature i) on the model output $v(N)$ is allocated based on their marginal contribution [58]. Based on several axioms to help allocate the contribution of each feature, shapely values are determined through:

$$\varphi_i = \sum_{S \subseteq N \setminus \{i\}} \frac{|S|!(n-|S|-1)!}{n!} [v(S \cup \{i\}) - v(S)] \quad (1)$$

A linear function of binary features g is defined based on the following additive feature attribution method:

$$g(z') = \varphi_0 + \sum_{i=1}^M \varphi_i z'_i \quad (2)$$

Where $z' \in [1]M$, equals 1 when a feature is observed; otherwise, it equals 0, and M is the number of input features [55].

2.2.3. Polynomial Regression

Polynomial regression is a type of linear regression where the polynomial relation between variables is described by a curve instead of a straight line. Python's machine learning library "sklearn" was used to find a polynomial equation that fits our dataset. The dataset was split into training and testing data X and Y , respectively, then systematically varied the degree of the polynomial from 1st to 5th degree and captured the performance of each of the polynomials through multiple metrics (R square, mean square error, mean absolute percentage error, mean absolute error, and sum square error) for later comparisons with our ANN model.

3. Results and discussions

The architecture and training parameters that were chosen for the current model helped to rapidly reach a low loss of value, as shown in Fig 4. The training was stopped after 700 epochs when it reached a meager loss value and avoided overfitting. The trained model also showed impressive predictive capability, as illustrated in Fig 5, where the predicted values are relatively accurate.

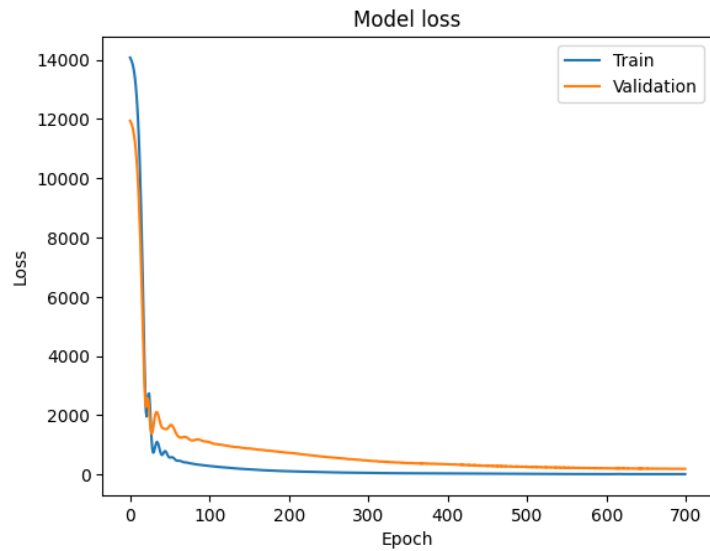


Fig 4: Predicted values of torque loss for training and validation datasets

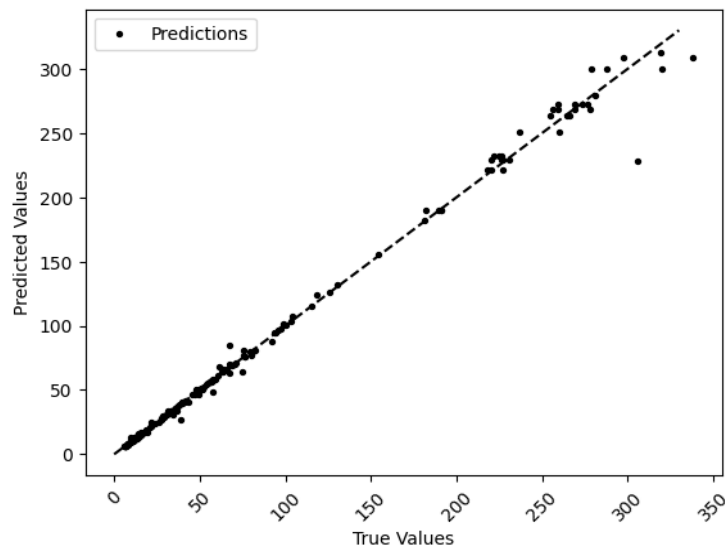


Fig 5: Predicted and experimental torque comparison

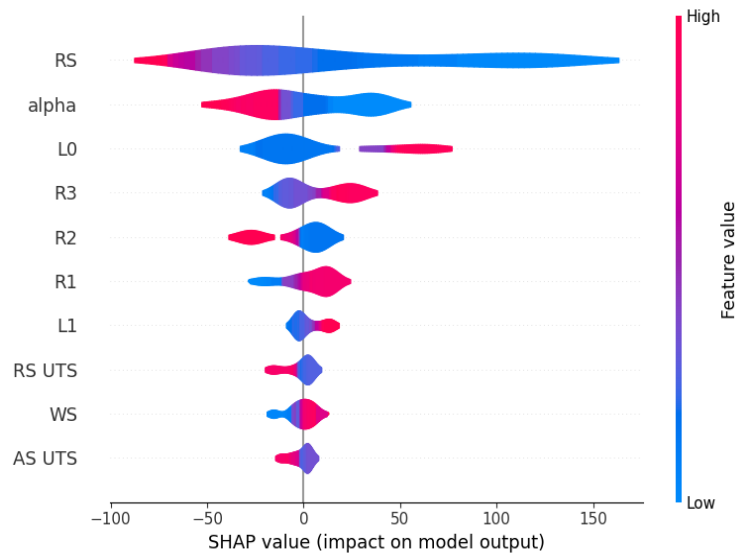
Several criteria were employed to assess the accuracy of the predictive model. The resulting R-squared of 99.53% can be referred to as the variability in torque requirements, which can be effectively attributed to the input parameters. This result underscores the model's robust explanatory capacity. The limited values of MAE = 4.38 indicated that the predicted torque does not deviate from the experimental sets. Moreover, the MAPE of 5.94% reflects its reliability in estimating torque requirements with a high degree of fidelity. Finally, the RMSE of 7.48 shows the precision of the predictions. The best results of the polynomial regression based on the previously mentioned metrics are of 2 then 1, respectively. As stated in Table 3, while the rest of the polynomial preformed worst. The comparisons show that the current ANN model performed better than the polynomial regression on testing data. Collectively, these metrics explain the outstanding performance of the model in predicting torque.

Table 3: Comparisons of polynomial regression and the modified ANN model

	Polynomial Regression		ANN model
	Degree = 1	Degree = 2	
MSE	473.64	280.08	55.87
R2	0.952	0.971	0.995
MAE	15.8	12.39	4.38
MAPE	56.86%	36.57%	5.94%
RMSE	21.76	16.74	7.48
SSE	2.75E+4	1.62E+4	4861.19

Using "SHAP" gives more precise indications about the parameters that most affect the torque used in the FSW process. Fig 6 shows that "Rotational Speed," "Plate thickness," and "Tilt angle" have a significant impact on torque predictions, which highlights their critical roles in FSW process control and optimization.

The Rotational speed (RS) was the most influential feature, with a mean absolute SHAP value of 52.71, emphasizing the importance of controlling rotational speed to optimize torque. It can be deduced from the SHAP graph that RS and torque have an inverse relationship. The Tilt Angle at 22.91 SHAP value plays a substantial role in torque generation and should be managed precisely. It can be deduced from the SHAP graph that tilt angle and torque have an inverse relationship. Plate Thickness at 22.43 SHAP value significantly affects torque, highlighting its role in design considerations. It can be deduced from the SHAP graph that Plate Thickness and torque have a direct relationship.

**Fig 6: SHAP values of predictive torque model**

4. Conclusions

Torque plays a vital role in friction stir welding studies, as it affects the quality of the weld and the efficiency of the weld joint. Machine learning is considered an effective tool in manufacturing operations. In this study, a machine learning model was prepared based on artificial neural networks and Shapley Additive Explanations. The current comprehensive study shows:

1. With a high R-squared score of 0.995, the predictive ANN model performs exceptionally well, explaining 99.53% of the variability in torque and establishing a benchmark for accuracy. Significantly low MAE, MAPE, and RMSE values (4.38, 5.94%, and 7.48) highlight its accuracy in torque prediction.

2. The study highlighted the pivotal roles played by "Rotational Speed," "Plate Thickness," and "tilt angle" in shaping torque predictions. These insights provide a foundation for informed decision-making in FSW process optimization, facilitating the fine-tuning of parameters to achieve desired torque values.
3. The study confirmed that combining predictive modeling and parameter importance analysis can achieve FSW optimization, which leads to reduced energy consumption.

5. Nomenclature

FSW	Friction Stir Welding
MAE	Mean Absolute Error
MAPE	Mean absolute Percentage Error
RMSE	Root Mean Square Error
ANN	Artificial Neural Network
MSE	Mean Square Error
SHAP	Shapley Additive exPlanations
SSE	Sum Square Error
RS	Rotational Speed
WS	Welding Speed (advancing speed)
AS TS	Advancing Side Tensile Strength
RS TS	Retreating Side Tensile Strength
L0	Plate Thickness
L1	Pin Length
R1	Shoulder Radius
R2	Pin base Radius
R3	Pin tip Radius
Alpha	Tilt angle
T	Torque

References

- [1] R. Gupta, D. Srivastava, M. Sahu, S. Tiwari, R. K. Ambasta, P. Kumar, Artificial intelligence to deep learning: machine intelligence approach for drug discovery, *Molecular diversity*, Vol. 25, pp. 1315-1360, 2021.
- [2] F. D. Kakhki, S. A. Freeman, G. A. Mosher, Evaluating machine learning performance in predicting injury severity in agribusiness industries, *Safety science*, Vol. 117, pp. 257-262, 2019.
- [3] H. R. Rohani Raftar, A. Parvizi, Prediction and optimization of load and torque in ring rolling process through development of artificial neural network and evolutionary algorithms, *Journal of Computational Applied Mechanics*, Vol. 49, No. 2, pp. 292-303, 2018.
- [4] D. Narciso, F. Martins, Application of machine learning tools for energy efficiency in industry: a review. *Energy Rep.* 6, 1181–1199 (2020).
- [5] A. Chandola, R. M. Pandey, R. Agarwal, L. Rathour, V. N. Mishra, On some properties and applications of the generalized m-parameter Mittag-Leffler function, *Adv. Math. Models Appl.*, Vol. 7, No. 2, pp. 130-145, 2022.
- [6] R. Outa, F. R. Chavarette, V. N. Mishra, A. C. Gonçalves, A. Garcia, S. da Silva Pinto, L. Rathour, L. N. Mishra, Analysis and Prognosis of Failures in Intelligent Hybrid Systems Using Bioengineering: Gear Coupling, *The Journal of Engineering and Exact Sciences*, Vol. 8, No. 1, pp. 13673-01-18e, 2022.
- [7] H. Tourajizadeh, S. Manteghi, S. Nekoo, Numerical and neural network modeling and control of an aircraft propeller, *Journal of Computational Applied Mechanics*, Vol. 49, No. 1, pp. 63-69, 2018.
- [8] N. T. Negero, G. F. Duressa, L. Rathour, V. N. Mishra, A novel fitted numerical scheme for singularly perturbed delay parabolic problems with two small parameters, *Partial Differential Equations in Applied Mathematics*, Vol. 8, pp. 100546, 2023.

- [9] M. Sharma, A. Sadhna, S. K. Bhargava, L. Rathour, L. N. Mishra, S. Pandey, A fermatean fuzzy ranking function in optimization of intuitionistic fuzzy transportation problems, *Advanced Mathematical Models & Applications*, Vol. 7, No. 2, pp. 191-204, 2022.
- [10] M. S. Hogeme, M. M. Woldaregay, L. Rathour, V. N. Mishra, A stable numerical method for singularly perturbed Fredholm integro differential equation using exponentially fitted difference method, *Journal of Computational and Applied Mathematics*, Vol. 441, pp. 115709, 2024.
- [11] M. Sharma, N. Dhiman, S. Kumar, L. Rathour, V. N. Mishra, Neutrosophic Monte Carlo simulation approach for decision making in medical diagnostic process under uncertain environment, *Int J Neutrosophic Sci*, Vol. 22, No. 1, pp. 08-16, 2023.
- [12] W. Cai, J. Wang, L. Cao, G. Mi, L. Shu, Q. Zhou, P. Jiang, Predicting the weld width from high-speed successive images of the weld zone using different machine learning algorithms during laser welding, *Math. Biosci. Eng.*, Vol. 16, No. 5, pp. 5595-5612, 2019.
- [13] K. Rameshkumar, A. Vignesh, P. G. Chandran, V. Kirubakaran, J. Sankaran, A. Sumesh, Machine learning models for weld quality monitoring in shielded metal arc welding process using arc signature features, *SAE International Journal of Materials and Manufacturing*, Vol. 15, No. 05-15-04-0023, pp. 347-365, 2022.
- [14] Z. Zhou, H. Shen, B. Liu, W. Du, J. Jin, Thermal field prediction for welding paths in multi-layer gas metal arc welding-based additive manufacturing: A machine learning approach, *Journal of Manufacturing Processes*, Vol. 64, pp. 960-971, 2021.
- [15] A. S. Bahedh, A. Mishra, R. Al-Sabur, A. K. Jassim, Machine learning algorithms for prediction of penetration depth and geometrical analysis of weld in friction stir spot welding process, *Metallurgical Research & Technology*, Vol. 119, No. 3, pp. 305, 2022.
- [16] B. Zhou, T. Pychynski, M. Reischl, E. Kharlamov, R. Mikut, Machine learning with domain knowledge for predictive quality monitoring in resistance spot welding, *Journal of Intelligent Manufacturing*, Vol. 33, No. 4, pp. 1139-1163, 2022.
- [17] H. Sun, P. Ramuhalli, R. E. Jacob, Machine learning for ultrasonic nondestructive examination of welding defects: A systematic review, *Ultrasonics*, Vol. 127, pp. 106854, 2023.
- [18] A. Chikh, M. Serier, R. Al-Sabur, A. Siddiquee, N. Gangil, Thermal Modeling of Tool-Work Interface during Friction Stir Welding Process, *Russian Journal of Non-Ferrous Metals*, Vol. 63, No. 6, pp. 690-700, 2022.
- [19] Z. Fu, D. He, H. Wang, Friction stir welding of aluminum alloys, *Journal of Wuhan University of Technology-Materials Science Edition*, Vol. 19, No. 1, pp. 61-64, 2004.
- [20] R. Al-Sabur, Tensile strength prediction of aluminium alloys welded by FSW using response surface methodology—Comparative review, *Materials Today: Proceedings*, Vol. 45, pp. 4504-4510, 2021.
- [21] W. H. Khalafe, E. L. Sheng, M. R. Bin Isa, A. B. Omran, S. B. Shamsudin, The Effect of Friction Stir Welding Parameters on the Weldability of Aluminum Alloys with Similar and Dissimilar Metals, *Metals*, Vol. 12, No. 12, pp. 2099, 2022.
- [22] A. Asmare, R. Al-Sabur, E. Messele, Experimental investigation of friction stir welding on 6061-T6 aluminum alloy using Taguchi-Based GRA, *Metals*, Vol. 10, No. 11, pp. 1480, 2020.
- [23] M. S. M. Isa, K. Moghadasi, M. A. Ariffin, S. Raja, M. R. bin Muhamad, F. Yusof, M. F. Jamaludin, N. bin Yusoff, M. S. bin Ab Karim, Recent research progress in friction stir welding of aluminium and copper dissimilar joint: a review, *Journal of Materials Research and Technology*, Vol. 15, pp. 2735-2780, 2021.
- [24] R. K. Al-Sabur, A. K. Jassim, Friction stir spot welding applied to weld dissimilar metals of AA1100 Al-alloy and C11000 copper, in *Proceeding of*, IOP Publishing, pp. 012087.
- [25] Y. Chen, J. Xie, W. Cao, Research on friction stir welded joints of Copper to Magnesium alloy, in *Proceeding of*, Atlantis Press, pp. 310-315.
- [26] S. Jana, Y. Hovanski, G. J. Grant, Friction stir lap welding of magnesium alloy to steel: a preliminary investigation, *Metallurgical and Materials Transactions A*, Vol. 41, pp. 3173-3182, 2010.
- [27] H. I. Khalaf, R. Al-Sabur, H. A. Derazkola, Effect of number of tool shoulders on the quality of steel to magnesium alloy dissimilar friction stir welds, *Archives of Civil and Mechanical Engineering*, Vol. 23, No. 2, pp. 125, 2023.
- [28] Y. Huang, X. Meng, Y. Xie, L. Wan, Z. Lv, J. Cao, J. Feng, Friction stir welding/processing of polymers and polymer matrix composites, *Composites Part A: Applied Science and Manufacturing*, Vol. 105, pp. 235-257, 2018.
- [29] R. Al-Sabur, M. Serier, A. Siddiquee, Analysis and construction of a pneumatic-powered portable friction stir welding tool for polymer joining, *Advances in Materials and Processing Technologies*, pp. 1-15, 2023.
- [30] H. Aghajani Derazkola, N. Kordani, R. Mohammadi Abokheili, Investigation of joining mechanism of electrical-assist friction stir joining between polyethylene (PE) and 316 stainless steel, *Archives of Civil and Mechanical Engineering*, Vol. 22, No. 4, pp. 1-13, 2022.

- [31] S. Senthil, M. Bhuvanesh Kumar, M. S. Dennison, A Contemporary Review on Friction Stir Welding of Circular Pipe Joints and the Influence of Fixtures on This Process, *Advances in Materials Science and Engineering*, Vol. 2022, 2022.
- [32] M. Costa, D. Verdera, J. Costa, C. Leitao, D. Rodrigues, Influence of pin geometry and process parameters on friction stir lap welding of AA5754-H22 thin sheets, *Journal of Materials Processing Technology*, Vol. 225, pp. 385-392, 2015.
- [33] S. Cui, Z. Chen, J. Robson, A model relating tool torque and its associated power and specific energy to rotation and forward speeds during friction stir welding/processing, *International Journal of Machine Tools and Manufacture*, Vol. 50, No. 12, pp. 1023-1030, 2010.
- [34] J. Qian, J. Li, J. Xiong, F. Zhang, W. Li, X. Lin, Periodic variation of torque and its relations to interfacial sticking and slipping during friction stir welding, *Science and Technology of welding and Joining*, Vol. 17, No. 4, pp. 338-341, 2012.
- [35] L. Shi, C. Wu, Z. Sun, An integrated model for analysing the effects of ultrasonic vibration on tool torque and thermal processes in friction stir welding, *Science and Technology of Welding and Joining*, Vol. 23, No. 5, pp. 365-379, 2018.
- [36] J. W. Pew, T. W. Nelson, C. D. Sorensen, Development of a torque-based weld power model for friction stir welding, *Friction Stir Welding and Processing IV*, pp. 73-82, 2007.
- [37] H. Su, C. S. Wu, A. Pittner, M. Rethmeier, Simultaneous measurement of tool torque, traverse force and axial force in friction stir welding, *Journal of Manufacturing processes*, Vol. 15, No. 4, pp. 495-500, 2013.
- [38] J. Yan, M. A. Sutton, A. P. Reynolds, Process–structure–property relationships for nugget and heat affected zone regions of AA2524–T351 friction stir welds, *Science and Technology of Welding and Joining*, Vol. 10, No. 6, pp. 725-736, 2005.
- [39] T. Long, W. Tang, A. P. Reynolds, Process response parameter relationships in aluminium alloy friction stir welds, *Science and technology of welding and joining*, Vol. 12, No. 4, pp. 311-317, 2007.
- [40] M. Costa, C. Leitão, D. Rodrigues, Parametric study of friction stir welding induced distortion in thin aluminium alloy plates: A coupled numerical and experimental analysis, *Thin-Walled Structures*, Vol. 134, pp. 268-276, 2019.
- [41] K. J. Quintana, J. L. L. Silveira, Mechanistic models and experimental analysis for the torque in FSW considering the tool geometry and the process velocities, *Journal of Manufacturing Processes*, Vol. 30, pp. 406-417, 2017.
- [42] K. J. Quintana, M. C. Fonseca, J. L. Silveira, Influence of Pin Shape Geometry on the Torque, Forces, and Residual Stresses in Friction Stir Welding of 5052-H34 Aluminum Alloy, *Soldagem & Inspeção*, Vol. 27, pp. e2710, 2022.
- [43] K. J. Quintana Cuellar, J. L. L. Silveira, Analysis of torque in friction stir welding of aluminum alloy 5052 by inverse problem method, *Journal of Manufacturing Science and Engineering*, Vol. 139, No. 4, pp. 041017, 2017.
- [44] A. Banik, J. Deb Barma, S. C. Saha, Effect of threaded pin tool for friction stir welding of AA6061-T6 at varying traverse speeds: torque and force analysis, *Iranian Journal of Science and Technology, Transactions of Mechanical Engineering*, Vol. 44, pp. 749-764, 2020.
- [45] A. Banik, B. S. Roy, J. D. Barma, S. C. Saha, An experimental investigation of torque and force generation for varying tool tilt angles and their effects on microstructure and mechanical properties: Friction stir welding of AA 6061-T6, *Journal of Manufacturing Processes*, Vol. 31, pp. 395-404, 2018.
- [46] C. Jonckheere, B. de Meester, A. Denquin, A. Simar, Torque, temperature and hardening precipitation evolution in dissimilar friction stir welds between 6061-T6 and 2014-T6 aluminum alloys, *Journal of materials processing technology*, Vol. 213, No. 6, pp. 826-837, 2013.
- [47] M. Reza-E-Rabby, A. P. Reynolds, Effect of tool pin thread forms on friction stir weldability of different aluminum alloys, *Procedia Engineering*, Vol. 90, pp. 637-642, 2014.
- [48] U. Acharya, B. S. Roy, S. C. Saha, Torque and force perspectives on particle size and its effect on mechanical property of friction stir welded AA6092/17.5 SiCp-T6 composite joints, *Journal of Manufacturing Processes*, Vol. 38, pp. 113-121, 2019.
- [49] P. Upadhyay, A. P. Reynolds, Effects of thermal boundary conditions in friction stir welded AA7050-T7 sheets, *Materials Science and Engineering: A*, Vol. 527, No. 6, pp. 1537-1543, 2010.
- [50] V. Buchibabu, G. Reddy, A. De, Probing torque, traverse force and tool durability in friction stir welding of aluminum alloys, *Journal of Materials Processing Technology*, Vol. 241, pp. 86-92, 2017.
- [51] M. Mehta, A. Arora, A. De, T. DebRoy, Tool geometry for friction stir welding—optimum shoulder diameter, *Metallurgical and Materials Transactions A*, Vol. 42, pp. 2716-2722, 2011.

- [52] M. Peel, A. Steuwer, P. Withers, T. Dickerson, Q. Shi, H. Shercliff, Dissimilar friction stir welds in AA5083-AA6082. Part I: Process parameter effects on thermal history and weld properties, *Metallurgical and Materials Transactions A*, Vol. 37, pp. 2183-2193, 2006.
- [53] H. Jia, K. Wu, Y. Sun, F. Hu, G. Chen, Evaluation of axial force, tool torque and weld quality of friction stir welded dissimilar 6061/5083 aluminum alloys, *CIRP Journal of Manufacturing Science and Technology*, Vol. 37, pp. 267-277, 2022.
- [54] S. Agatonovic-Kustrin, R. Beresford, Basic concepts of artificial neural network (ANN) modeling and its application in pharmaceutical research, *Journal of pharmaceutical and biomedical analysis*, Vol. 22, No. 5, pp. 717-727, 2000.
- [55] S. M. Lundberg, S.-I. Lee, A unified approach to interpreting model predictions, *Advances in neural information processing systems*, Vol. 30, 2017.
- [56] E. Štrumbelj, I. Kononenko, Explaining prediction models and individual predictions with feature contributions, *Knowledge and information systems*, Vol. 41, pp. 647-665, 2014.
- [57] M. T. Ribeiro, S. Singh, C. Guestrin, " Why should i trust you?" Explaining the predictions of any classifier, in *Proceeding of*, 1135-1144.
- [58] Y. J. Levy, E. Solan, Stochastic games, *Complex Social and Behavioral Systems: Game Theory and Agent-Based Models*, pp. 229-250, 2020.